

# A probabilistic solar irradiance interval-valued prediction model with multi-objective optimization of reliability, sharpness and stability

Xueli Zhang\*

*School of Computer Science and Engineering,  
South China University of Technology,  
Guangzhou, China  
sherryiszx1@outlook.com*

Chun Sing Lai\*

*School of Automation,  
Guangdong University of Technology,  
Guangzhou, China  
chunsing.lai@brunel.ac.uk*

Wing W. Y. Ng\*

*School of Computer Science and Engineering,  
South China University of Technology,  
Guangzhou, China  
wingng@scut.edu.cn*

Shichao Xu

*School of Computer Science and Engineering,  
South China University of Technology,  
Guangzhou, China  
sc\_xu@foxmail.com*

Xiaomei Wu

*School of Automation,  
Guangdong University of Technology,  
Guangzhou, China  
epxm\_wu@gdut.edu.cn*

Jianjun Zhang

*School of Computer Science and Engineering,  
South China University of Technology,  
Guangzhou, China  
jjzhangscut@gmail.com*

Keda Pan

*School of Automation,  
Guangdong University of Technology,  
Guangzhou, China  
111904017@mail2.gdut.edu.cn*

Ting Wang

*Department of Radiology Guangzhou First People's Hospital,  
School of Medicine, South China University of Technology,  
Guangzhou, China  
tingwang@ieee.org*

Zhuoli Zhao

*School of Automation,  
Guangdong University of Technology,  
Guangzhou, China  
zhuoli.zhao@gdut.edu.cn*

Loi Lei Lai

*School of Automation,  
Guangdong University of Technology,  
Guangzhou, China  
l.l.lai@ieee.org*

**Abstract**—Improved interval-valued prediction models for solar power and irradiance forecasting allow enhanced planning and operation of solar power systems. Highly uncertain atmospheric and environmental factors are major challenges of solar irradiance forecasting. Existing upper and lower bound estimation methods mainly focus on narrowing the prediction intervals and minimizing forecasting errors. However, the sensitivity of the interval-valued prediction model is not considered. Sensitivity is described as the model's output fluctuations due to unseen samples. Models with high sensitivity may not perform well in real-life applications under uncertain environments. This paper presents a novel interval-valued prediction model, P\_RSS, by simultaneously optimizing the reliability, sharpness, and stability (RSS) for probabilistic solar irradiance interval-valued prediction. With sensitivity regularization, P\_RSS has reduced sensitivity to unseen samples with perturbations from training samples and enhanced robustness. An Extreme learning

machine (ELM) model is constructed to directly output prediction intervals (PIs) of solar irradiance via a multi-objective optimization of the RSS. An evaluation framework is proposed to verify the RSS performance. Moreover, a new comprehensive evaluation indicator is proposed to evaluate the PIs. Case studies on three American solar irradiance datasets show that P\_RSS yields outstanding performance against state-of-the-art methods.

**Index Terms**—Solar energy forecasting, prediction intervals, multi-objective optimization, sensitivity regularization.

## I. INTRODUCTION

Renewable energy generation plays a critical role in providing a sustainable future. Solar energy will have a prominent share in the future renewable energy mix to meet the global energy agenda to promote smart living, and to facilitate a low-carbon economy. And photovoltaic

\* denotes corresponding authors.

(PV) continuously increasing its share in the global power generation industry [1]. However, the intermittency of solar resource poses significant difficulties in the operation and planning of solar power systems within a smart grid.

Many recent works utilize statistical and Artificial intelligence models for solar irradiance and PV power estimation/regression problems. An overview is given as follows:

1) The studies of highly nonlinear regression methodologies including k-means clustering algorithm [2], [3], autoregressive integrated moving average (ARIMA) [4], artificial neural network (ANNs) [5], SVM regression models [6], least squares support vector machines (LS-SVM) [7], and optimal LS-SVM models [8].

2) Artificial intelligence (AI) models play an important role in solar energy prediction [9]. An adaptive learning hybrid model (ALHM) [10] is proposed by integrating time-varying multiple linear model (TMLM), genetic algorithm (GA) back propagation neural network (GABP) and the adaptive learning online hybrid algorithm. [11] propose a convolutional graph autoencoder to provide probabilistic forecasts of future solar irradiance. The problem of spatio-temporal solar irradiance forecasting is presented as a graph distribution learning problem.

In this paper, ELM is utilized to construct PIs which directly outputs the upper and lower bound of PIs. ELM has advantages of less learning parameters, fast training speed, and strong generalization ability [12], but it has the downside of low generalization capability [11]. To overcome the drawback of ELM, we utilize the stochastic sensitivity (STSM) to achieve a low generalization error for future unseen sample. Also, STSM improves the forecasting performance by considering the following features:

**Sensitivity:** The model's output fluctuations to unseen samples with small differences (perturbations) from training samples [13].

**Stability:** The model is stable enough to minimize forecasting errors due to unseen samples, with strong generalization ability and low sensitivity [13].

**Reliability:** The reliability measures the probability of the true values lie in the PIs, which is usually evaluated by the value of prediction interval coverage probability (PICP) [9], [14].

**Sharpness:** The width of prediction interval coverage [15].

**Robustness:** The model is insensitive to the influence of noise or minor disturbance [16].

Moreover, these LUBE-based methods [17] all focus on narrower interval width and higher accuracy only without considering the sensitivity of the model itself. Some error evaluation metrics will not optimize the prediction interval, but more improve the performance of point prediction, such as RMSE [18]. Some methods [17], [19], [14], [15], [20], [21] assess the performance of intervals by PICP or prediction interval normalized average width (PINAW), etc., ignore sensitivity. Multi-objective particle swarm optimization approach as described in [9] only simultaneously optimizes two goals, i.e., closeness to the target PIs nominal confidence

and the interval width of the upper and lower limits of the PIs.

Therefore, in this paper, in addition to the width (sharpness) and accuracy (reliability), sensitivity is considered for robust forecasting. A multi-objective optimization algorithm is utilized to train the neural network by optimizing these three objectives (RSS). Moreover, this paper presents a comprehensive evaluation indicator without artificial weight distribution to evaluate the quality of the interval-valued prediction model. Moreover, a technique of pre-training then adjusting is used to narrow the searching range of the optimization algorithm and to improve the algorithm efficiency. After that, non-dominating sorting genetic algorithm III (NSGA3) [22] was used to train the ELM, optimizing the RSS. The major contributions of this work are:

- 1) A multi-objective optimization method is applied to optimize the three objectives reliability, sharpness and sensitivity simultaneously to achieve better generalization ability and more accurate prediction interval. The key advantage is that the three objectives are optimized in a vector form, such that the selection of weights for different objectives is not required before applying the optimization. The final solution is selected from the Pareto front which consists of a set of non-dominating optimal solutions.
- 2) A new evaluation framework for RSS is proposed to train ELM-based PIs model with higher generalization capabilities. The RSS evaluates a PIs model in three aspects: reliability, sharpness and sensitivity. In contrast to traditional LUBE-based PIs learning which optimizes the reliability and sharpness only, the optimization of sensitivity in RSS enhances the robustness of the network for future unseen samples with minor differences from training samples.
- 3) A comprehensive evaluation indicator is proposed to evaluate the interval-valued prediction results. This indicator has the advantage of without assigning weights to the model's sharpness and reliability, which is suitable for the multi-objective optimization problem.
- 4) Extensive experiments are carried out to confirm the superiority of P\_RSS. P\_RSS greatly reduces the width of the prediction interval, by only losing a small amount of prediction accuracy.

## II. RSS EVALUATION FUNCTIONS

The solar irradiance interval-valued prediction model forecasts the solar irradiance of the next timestamp and gives a prediction interval with a certain degree of confidence. One of the goals of constructing the prediction interval is to keep it as reliable and as sharp as possible. Therefore, measures to evaluate the accuracy and width of the prediction interval are necessary. These two measures had been reported in many studies of interval-valued prediction [23], [24], [25]. Models that produce stable results with a training set may perform better in test sets or in practical applications, where high uncertainty may be encountered due to various factors [22].

Therefore, in addition to reliability and sharpness, sensitivity is also considered in the P<sub>RSS</sub>.

### A. Reliability and Sharpness

This paper employs PICP to assess the reliability of the model's performance, which can be evaluated by calculating the probability that the target solar irradiance falls within the PIs.

$$PICP = \frac{1}{N} \sum_{i=1}^N c_i \quad (1)$$

$$c_i = \begin{cases} 0 & Y_i \notin [L_i, U_i] \\ 1 & Y_i \in [L_i, U_i] \end{cases} \quad (2)$$

where  $N$  is the number of samples,  $Y_i$  is the target solar irradiance, and  $L_i, U_i$  are the lower bound and upper bound of prediction interval respectively.

In general, higher PICP is preferred. But in a practical situation, a common practice is to achieve a prescribed probability  $(1 - \alpha)$ , named PINC. Therefore, we propose an evaluation function  $R$  to adapt to this situation as follows:

$$R = \max((1 - \alpha) - PICP, 0) \quad (3)$$

When PICP is lower than given PINC  $(1 - \alpha)$ ,  $R = \max((1 - \alpha) - PICP, 0)$ , when PICP is greater than  $(1 - \alpha)$ ,  $R = 0$ . A lower  $R$  means stronger reliability of the given prediction interval.

It is important to note that the PICP may not achieve the PINC  $(1 - \alpha)$ . Even if the PICP achieves PINC on the training set, it maybe a little lower on testing set or in practical applications. Therefore, we do not rigidly require that the PICP be greater than  $(1 - \alpha)$  and only treat the PINC as a soft constraint.

When the interval covers the entire range of solar irradiance, we can get a 100% PICP. However, this interval is meaningless. We cannot get any information about future solar irradiance. Therefore, an evaluation criterion to control the width of the interval is needed, i.e., the prediction interval average width (PIAW):

$$PIAW = \frac{1}{N} \sum_{i=1}^N (U_i - L_i) \quad (4)$$

If the range of solar irradiance is known, then the prediction interval normalized average width (PINAW) could be calculated as:

$$PINAW = \frac{1}{N \times r} \sum_{i=1}^N (U_i - L_i) \quad (5)$$

where  $r$  is the maximum value of solar irradiance in each data set.

In addition to simply considering the width of the interval, a penalty function  $P_i$  is included for the deviation of the prediction interval from the target solar irradiance:

$$c_i = \begin{cases} Y_i - L_i & Y_i < L_i \\ 0 & Y_i \in [L_i, U_i] \\ U_i - Y_i & Y_i > U_i \end{cases} \quad (6)$$

When the target solar irradiance falls within the PIs,  $P_i = 0$ , otherwise,  $P_i$  equals the distance from the target solar irradiance to the PIs boundary.

By combining *PINAW* and penalty function  $P_i$ , we propose an evaluation function *SharpScore* to evaluate sharpness:

$$SharpScore = \frac{1}{N \times r} \sum_{i=1}^N (U_i - L_i + \mu P_i) \quad (7)$$

where  $\mu$  is a penalty coefficient.

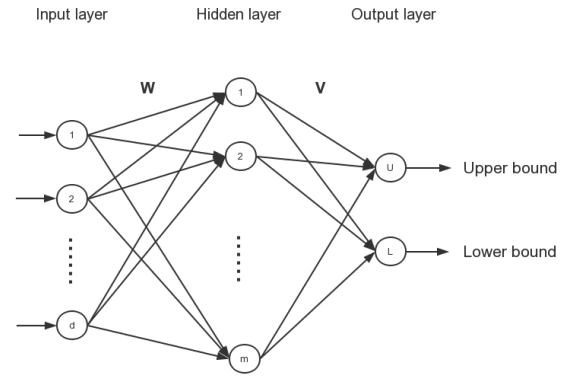


Fig. 1. The structure of ELM.

### B. Stability

The training process should produce a stable model for better generalization capabilities. Therefore an indicator to evaluate the sensitivity of the model is necessary. The sensitivity of P<sub>RSS</sub> is measured by the stochastic sensitivity (STSM) derived from [26]. The STSM has been widely applied in different applications, for instances, neural network architecture selection [27], sample selection [28], time sequence forecasting [29] and multilayer perceptron neural network (MLPNN) training [26]. The STSM of a model  $f$  is computed by the average output deviations yielded by small perturbations to its input features:

$$E_{S_Q} [(\Delta y)^2] = \frac{1}{N} \sum_{i=1}^N E [(f(x_i + \Delta x) - f(x_i))^2] \quad (8)$$

where  $x_i$  is a  $d$ -dimension input of model  $f$ ,  $\Delta x \in [-Q, Q]^d$  denotes the perturbation within a distance of  $Q$  in each dimension of the input features,  $\Delta y$  is the output perturbation of model  $f$ , and  $E()$  is the expectation operator. In this work, P<sub>RSS</sub> would output upper bound and lower bound at the same time, which means model  $f$  would return a 2-dimensional vector. Therefore, we propose STSM for multi-dimensional output:

### III. SOLAR IRRADIANCE INTERVAL-VALUED PREDICTION VIA RSS

$$STSM = E_{S_Q} [(\Delta y)^2] = \frac{1}{N} \sum_{i=1}^N E [\|f(x_i + \Delta x) - f(x_i)\|^2] \quad (9)$$

where  $\|\cdot\|$  means the 2-norm of a vector.

A quasi-Monte-Carlo-based method is used to calculate STSM.  $\Delta x$  is generated via an n-dimensional Halton sequence [30] with each coordinate ranging from  $[-Q, Q]$ . In P\_RSS, 30 Halton points are used in the calculation of the expectation term in Equation(9).

Finally, three objective functions (3), (7) and (9) are obtained. The solar irradiance interval-valued prediction problem is turned into a multi-objective optimization problem:

Objectives: Build an optimal model to:

Minimize: SharpScore, STSM, R.

#### C. Comprehensive Evaluation Indicator

The goal is to build a solar irradiance interval-valued prediction model with high reliability, sharpness, and stability. A stable model will eventually be able to construct narrower and more accurate PIs on test data with high uncertainty. Therefore, we would evaluate PIs by PICP and PINAW. It is difficult to identify the optimal result by using multiple metrics at the same time. For example, a model with higher accuracy but wider width and the other with lower accuracy but narrower width. Therefore, many previous studies had proposed their comprehensive indicators to integrate reliability and sharpness [23], [24], [25]. However, these indicators all require explicit or implicit weight distribution of the two objectives. Here, we propose a new evaluation indicator that does not require any weighing on PICP and PINAW:

$$CEI = \max(1 - PICP, \alpha) \times PINAW + \rho(\max(0.5 - PICP, 0) + \max(PINAW - 0.75, 0)) \quad (10)$$

Where  $\alpha$  comes from the PINC  $(1 - \alpha)$ .  $\rho$  is a penalty coefficient, which should be selected to have a large value, like 10000. The lower CEI stands for a better model result. When the result becomes better (higher PICP, lower PINAW), the CEI would become lower, or vice versa. The part  $\max(1 - PICP, \alpha)$  will let CEI focus on PINAW when PICP reaches PINC. This multiplication form eliminates the problem of weight distribution. No matter how the weights are assigned, there will be no change in the evaluation results but just multiply a constant. Besides, we believe that results with  $PICP < 50\%$  or  $PINAW > 75\%$  are unacceptable, which are not practical. Therefore, we introduce a penalty term (the right part in CEI). When  $PICP < 50\%$  or  $PINAW > 75\%$ , CEI will increase significantly, and also avoid the abnormal situation that CEI will get the minimum value 0 when  $PINAW = 0$ .

P\_RSS is adopted for training an MLP for constructing PIs by NSGA3 algorithm. It consists of two major components: ELM pre-training and multi-objective optimization.

#### A. ELM Pre-training

If we use optimization algorithm on MLP directly, the quality and efficiency of the underlying optimization might be negatively affected by a large number of model parameters [23]. ELM is a single hidden-layer feedforward neural network, which randomly chooses the input weights and analytically determines the output weights [31]. It greatly reduces the number of parameters that need to be optimized because the first layer weights are randomly assigned, which do not participate in the learning step. The ELM structure used in this article is shown in Fig. 1. The activation function of hidden units is  $\phi(x) = \frac{1}{1+e^x}$ , the activation function of output units is a linear function  $l(x) = x$ . Given an input vector  $x$ , the output value of hidden unit  $j$  is:

$$O_j(x) = \phi\left(\sum_{i=1}^d w_{i,j}x_i + b_j\right) \quad (11)$$

where  $w_{i,j}$  is the weight from input unit  $i$  to hidden unit  $j$ ,  $b_j$  is the bias of hidden unit  $j$ . For an ELM with  $m$  hidden units, we can get the output matrix  $H$  of the hidden layer as below:

$$H = \begin{pmatrix} O_1(x) \\ \vdots \\ O_m(x) \end{pmatrix} \quad (12)$$

For a set of input vectors  $X = (x^{(1)}, x^{(2)}, \dots, x^{(N)})$ , the output matrix  $H$  would be

$$H = \begin{bmatrix} O_1(x^{(1)}) & \dots & O_1(x^{(N)}) \\ \vdots & \ddots & \vdots \\ O_m(x^{(1)}) & \dots & O_m(x^{(N)}) \end{bmatrix} \quad (13)$$

Then the output of the ELM would be

$$\begin{pmatrix} U \\ L \end{pmatrix} = VH \quad (14)$$

where  $V$  is a  $2 \times m$  matrix, which represents the weight from the hidden layer to the output layer.  $W$  represents the weight from the input layer to the hidden layer in Fig. 1. By randomly chooses the input weights, the matrix  $H$  has been determined. Therefore, the problem becomes to optimize the matrix  $V$  in Equation (14).

Since optimization algorithms are essentially search strategies [22], if the range is too large, it may harm search efficiency and quality of results. In our method, the range of matrix  $H$  would be  $R_{m \times N}$ . A pre-training then adjusting method is proposed to reduce the search range. Since the activation function of the output layer is a linear activation function, and the upper and lower bounds of the output

values should be near the target solar irradiance, we can first set the target output values  $L$  and  $U$  to the target solar irradiance  $Y$ , that is  $\begin{pmatrix} U \\ L \end{pmatrix} = VH$ . This will get the pre-training matrix  $V$  by solving this equation according to the least-squares method. After that, we introduce an adjustment matrix  $G \in [-1, 1]_{m \times n}$ , let  $V^* = V + G * V$ , where  $G * V$  denotes the Hadamard product of  $G$  and  $V$ . The final model output should be  $\begin{pmatrix} U \\ L \end{pmatrix} = V^* H$ . Thus our optimization parameter object becomes matrix  $G$  and its range is  $[-1, 1]_{m \times n}$ .

### B. Multi-objective Optimization

After pre-training the ELM, all parameters of P\_RSS have been determined except for matrix  $G$ . Here, a multi-objective optimization algorithm NSGA3 is performed to optimize the matrix  $G$  by minimizing SharpScore, STSM and R. The flowchart is shown in Fig. 2.

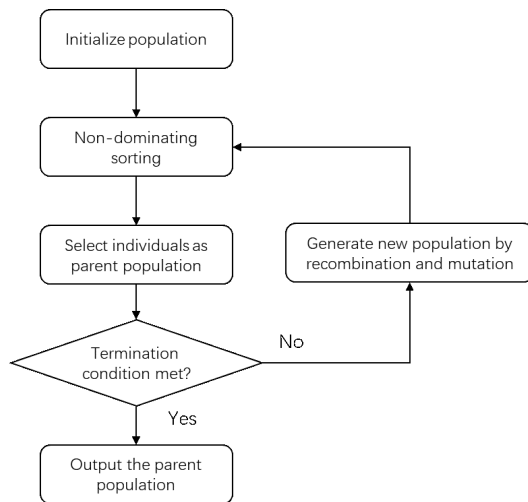


Fig. 2. The Flowchart of NAGA3.

The NSGA3 optimization algorithm used in P\_RSS can be described in the following 5 steps:

#### S1. Initialize population

Randomly generate an initial population, where in each individual represents a candidate matrix  $G$ .

#### S2. Non-dominating sorting

For each individual, the upper bounds and lower bounds of prediction interval are calculated by the ELM model, and then Sharpness, STSM and R can be further calculated. After that, nondominating sort individuals in population base on their Sharpness, STSM and R values, and divide individuals into multiple ordered nondominated layers.

#### S3. Select parent population

Firstly, create an empty parent population which can contain  $N$  individuals. Consequently, add the individuals in the top ranked non-dominated layers to the parent population in turn, until the limit is reached. For the last included nondominated layers, not all individuals

can be selected to join the parent population. In this situation, in order to satisfy the individual's diversity, a reference point-based method [22] is used for individual selection.

#### S4. Check termination criteria

If the iteration reaches the limit, output the Pareto optimality solutions (individuals belonging to the first non-dominated layers) in parent population as results, otherwise perform S5.

#### S5. Generate new population

Generate child population by recombination and mutation [22] from parent population, and then combine it with parent population as a new population. After that, go to S2.

As a result, a set of Pareto optimality solutions is obtained. It is hypothesized that the solutions obtained with the multi-objective optimization algorithm are relatively stable. This is because one of the objectives is to minimize STSM. Therefore, we focus on the reliability and sharpness, use CEI to evaluate these solutions and pick the solution with the smallest CEI as our final prediction model.

TABLE I  
PARAMETER VALUES

Parameters	Values
Significance Level $\alpha$	0.1
Q	0.01
Penalty Coefficient $\rho$	4
Number of Hidden Units	30
Maximum Number of Iterations	200
Population Size	100
Crossover Percentage	0.5
Mutation Percentage	0.5
Mutation Rate	0.04

TABLE II  
PERFORMANCE OF THE PROPOSED METHOD ON A DIFFERENT NUMBER OF HIDDEN UNIT FOR USADATA-1.

Hidden Units	PICP[%]	PINAW[%]	CEI
10	90.63	43.37	0.0434
20	89.79	31.31	0.0320
30	89.10	27.47	0.0300
40	89.03	28.00	0.0307
50	88.98	35.74	0.0394

## IV. EXPERIMENTS

Three sets of USA solar irradiance data and weather data from National Renewable Energy Laboratory (<https://www.nrel.gov/gis/data-tools.html>) [32] are used to evaluate the effectiveness of the proposed method. The latitude and longitude of these three datasets are 30.25°N 81.86°W, 41.45°N 84.46°W, and 41.17°N 75.42°W respectively. Data from 1st Jan 2010 to 31st Dec 2017 consist of sampling frequency to be 30min/sample. Data from 1st Jan 2010 to 31st Dec 2016 are used for training and the rest for testing. The collected data consists of 7 features, including timestamp, temperature (°C), relative humidity (%), wind speed (m/s), dew point (°C), global horizontal irradiance (GHI)

( $W/m^2$ ), and clear sky GHI ( $W/m^2$ ). Some data processing steps like normalization, feature difference (new features are obtained by subtracting the corresponding features from half an hour ago), feature intersection and feature selection are performed before the half-hour-ahead prediction. Also, data before sunrise have been removed. PICP and PINAW in Equations (1) and (5) are used to evaluate accuracy and interval width, respectively. CEI in Equation (10) is the comprehensive evaluation indicator of the model.

The experiment is designed to compare the proposed method with other methods, including lower upper bound estimation method (LUBE) [23], optimal granule-based PIs construction method (OGPIC) [33] and two particle swarm optimization (PSO) based methods (MLP-PSO and MLP-MOPSO) from [9]. Follow the suggestions from [22] and [33], parameters of the proposed method are shown in Table I. All methods share the same PINC, number of hidden units, and population size. PSO based methods would have a higher maximum number of iterations like 2000.

Firstly, we analyze the effect of using a different number of hidden layer units. Table II summarizes the PICP, PINAW, STS and CEI results for the proposed method with a various number of hidden layer units from 10 to 50. Table II shows that as the number of hidden layer units changes from 10 to 50, CEI becomes lower and then higher, and the network with 30 hidden units performs best with the lowest CEI. On one hand, as the number of hidden units increases, the ELM becomes more complex, and its performance should be better 58. On the other hand, the increase in complexity means that NSGA3 needs to optimize more parameters and it is more difficult to find a better solution. The experiment in Table II shows that 30 hidden units could balance these two points and achieve a good result.

Secondly, we construct a comparative experiment on the effectiveness of RSS-based multi-objective optimization. The comparison method used is the same as the method except that genetic algorithm (GA) is used for single-objective optimization with CEI as the objective function. The result is shown in Table III. It can be seen that the proposed RSS-based multi-objective optimization algorithm is better than the single-objective optimization algorithm on all three data sets, which proves the effectiveness of the proposed method. Also, the proposed method behaves differently on 3 datasets, and obtains the highest PICP on USAdata-3. This is because solar irradiance would be affected by geographical location and climate change. USAdata-3 is located in the center of the United States, far from the ocean, and has less rainfall, so the accuracy of the solar irradiance prediction will be higher.

Table IV shows the experimental result on three datasets yielded by LUBE, OGPIC, MLP-PSO, MLP-MOPSO, and the proposed method. The proposed method yields the minimum value on CEI in all three datasets, i.e., the proposed method performs the best on all three data sets. Also, the proposed method achieves minimum values on PINAW of all three datasets. Compared to MLP-MOPSO, the proposed method is 21.20%, 18.43%, 30.92% narrower on PINAW and only takes the expense of 1.96%, 1.78%, 0.23% on PICP in

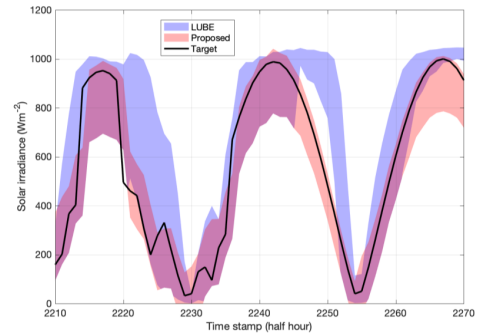


Fig. 3. Proposed method (P\_RSS) vs LUBE for USAdata-1.

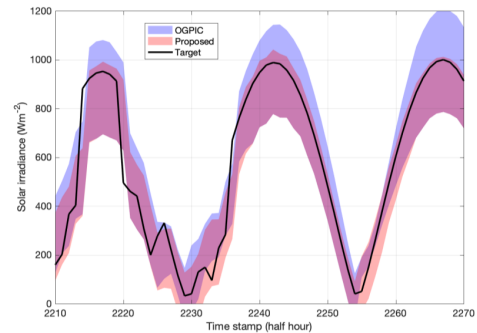


Fig. 4. Proposed method (P\_RSS) vs OGPIC for USAdata-1.

all three datasets respectively. It can be seen that the PIs given by proposed method exchanges a large improvement on PINAW at the expense of a small amount of PICP to get a better overall result. Besides, Tables V and VI show the comparison of results for different seasons for USAdata-1. Compared to other methods, the proposed method yields the lowest CEI among five comparison methods in all four seasons. Therefore, the proposed method is more robust to different seasons. Compared to LUBE, the proposed method can decrease the PINAW by 35.11%, 30.15%, 48.41% and 43.33% in Spring, Summer, Autumn and Winter, respectively. Besides that, the proposed method yields large PINAW in Summer. It is reasonable because poor weather conditions (e.g. showers) occur in summer. Fig. 3 to Fig. 6 show the comparison between the proposed method with LUBE, OGPIC, MLP-PSO and MLP-MOPSO for USAdata-1 respectively. The ordinate is the solar irradiance, and the abscissa is the timestamp from 1st Jan 2010 (half-hour per stamp). These figures show that the PIs provided by P\_RSS yield a less interval width than other methods, which is consistent with the results given in Table IV.

## V. CONCLUSION

This paper presents a novel solar irradiance interval-valued prediction model, P\_RSS, that reduces sensitivity to unseen samples and enhances the robustness of model with high generalization capabilities. An evaluation framework is developed to evaluate the reliability, sharpness and sensitivity

TABLE III  
COMPARISON BETWEEN MULTI-OBJECTIVE METHOD AND SINGLE OBJECTIVE METHOD.

Objectives	USAdata-1			USAdata-2			USAdata-3		
	PICP [%]	PINAW [%]	CEI	PICP [%]	PINAW [%]	CEI	PICP [%]	PINAW [%]	CEI
Multiple: RSS	89.10	27.47	0.0300	88.62	24.92	0.0284	91.60	30.40	0.0304
Single: CEI	89.27	29.99	0.0322	88.73	30.40	0.0343	90.79	32.42	0.0324

TABLE IV  
THE FORECASTING PERFORMANCE OF VARIOUS METHODS FOR THREE DATASETS.

Method	USAdata-1			USAdata-2			USAdata-3		
	PICP[%]	PINAW[%]	CEI	PICP[%]	PINAW[%]	CEI	PICP[%]	PINAW[%]	CEI
LUBE	88.78	39.37	0.0442	89.16	38.89	0.0422	90.53	35.85	0.0359
OGPIC	87.82	28.49	0.0347	89.88	31.66	0.0320	90.73	36.94	0.0369
MLP-PSO	90.00	45.94	0.0459	89.40	38.82	0.0411	89.30	38.84	0.0392
MLP-MOPSO	90.88	34.86	0.0358	90.23	30.55	0.0306	91.81	44.01	0.0440
P_RSS	89.10	27.47	0.0300	88.62	24.92	0.0284	91.60	30.40	0.0304

TABLE V  
RESULTS COMPARISON FOR USADATA-1 IN SPRING AND SUMMER.

Method	Spring			Summer		
	PICP[%]	PINAW[%]	CEI	PICP[%]	PINAW[%]	CEI
LUBE	89.92	39.28	0.0396	87.47	42.62	0.0534
OGPIC	85.81	26.26	0.0373	89.97	32.86	0.0330
MLP-PSO	94.42	54.30	0.0564	89.03	44.41	0.0487
MLP-MOPSO	91.48	39.29	0.0393	89.52	34.07	0.0357
P_RSS	87.67	25.49	0.0314	89.29	29.77	0.0319

TABLE VI  
COMPARISON RESULTS FOR USADATA-1 IN AUTUMN AND WINTER.

Method	Autumn			Winter		
	PICP[%]	PINAW[%]	CEI	PICP[%]	PINAW[%]	CEI
LUBE	88.55	46.32	0.0530	89.14	45.92	0.0499
OGPIC	88.65	30.10	0.0342	86.58	23.74	0.0319
MLP-PSO	85.74	40.40	0.0576	90.87	43.60	0.0436
MLP-MOPSO	89.99	34.28	0.0343	92.94	35.21	0.0352
P_RSS	87.58	26.80	0.0332	91.09	26.02	0.0260

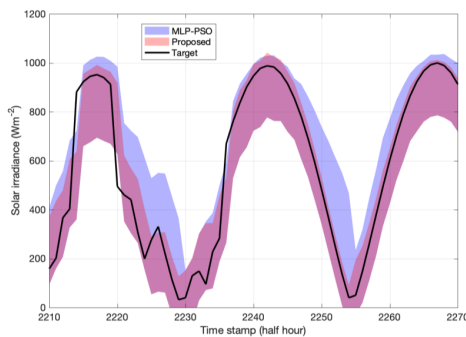


Fig. 5. Proposed method (P\_RSS) vs MLP-PSO for USAdata-1.

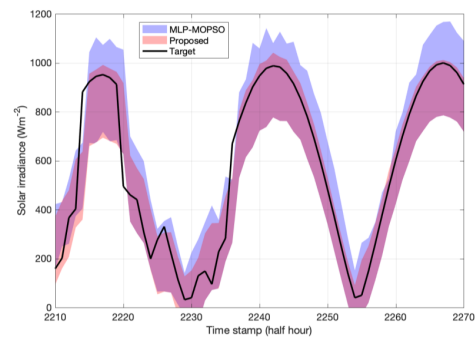


Fig. 6. Proposed method (P\_RSS) vs MLP-MOPSO for USAdata-1.

for model training. A multi-objective optimization method NSGA3 is used to train the pre-training ELM model. The method automatically tunes the model parameters by optimizing RSS without the need to select weights. Besides, a new evaluation indicator CEI is proposed to evaluate the interval prediction results for models using multi-objective optimization. Experiment results show that the proposed method performs better as compared to single-objective op-

timization models. Also, it has been determined that the proposed method yield the smallest CEI and PINAW values, based on case studies performed on with various data sets, seasons, and PINC values. It is worth mentioning that the proposed method sacrifices a small amount of PICP in exchange for a substantial decrease in PINAW, and ultimately provides the best overall result. The effectiveness of this interval-valued prediction model for improving other smart

grid applications including power demand forecasting and wind power prediction will be future work.

#### ACKNOWLEDGMENT

This work is supported by National Natural Science Foundation of China under Grants 61876066, 62206020, 61572201 and 51907031; Guangdong Province Science and Technology Plan Project (Collaborative Innovation and Platform Environment Construction) 2019A050510006; Guangzhou Science and Technology Plan Project 201804010245; Department of Finance and Education of Guangdong Province 2016 [202]: Key Discipline Construction Program, China; and the Education Department of Guangdong Province: New and Integrated Energy System Theory and Technology Research Group [Project Number 2016KCXTD022].

#### REFERENCES

- [1] Emilio Pérez, Javier Pérez, Jorge Segarra-Tamarit, and Hector Beltran. A deep learning model for intra-day forecasting of solar irradiance using satellite-based estimations in the vicinity of a pv power plant. *Solar Energy*, 218:652–660, 2021.
- [2] Enrica Scolarì, Fabrizio Sossan, and Mario Paolone. Irradiance prediction intervals for pv stochastic generation in microgrid applications. *Solar Energy*, 139:116–129, 2016.
- [3] Pingan Ni, Zengfeng Yan, Yingjun Yue, Liangliang Xian, Fuming Lei, and Xia Yan. Simulation of solar radiation on metropolitan building surfaces: A novel and flexible research framework. *Sustainable Cities and Society*, page 104469, 2023.
- [4] Yuxiang Cheng, Jiayu Yi, Xiaoguang Yang, Kin Keung Lai, and Luis Seco. A ceemd-arima-svm model with structural breaks to forecast the crude oil prices linked with extreme events. *Soft Computing*, 26(17):8537–8551, 2022.
- [5] Gabriel López, Christian A Gueymard, Juan Luis Bosch, Igor Rapp-Arrarás, Joaquín Alonso-Montesinos, Inmaculada Pulido-Calvo, Jesús Ballestrín, Jesús Polo, and Javier Barbero. Modeling water vapor impacts on the solar irradiance reaching the receiver of a solar tower plant by means of artificial neural networks. *Solar Energy*, 169:34–39, 2018.
- [6] Debaditya Chakraborty, Hazem Elzarka, and Raj Bhatnagar. Generation of accurate weather files using a hybrid machine learning methodology for design and analysis of sustainable and resilient buildings. *Sustainable Cities and Society*, 24:33–41, 2016.
- [7] Maria Malvoni, Maria Grazia De Giorgi, and Paolo Maria Congedo. Photovoltaic forecast based on hybrid pca-lssvm using dimensionality reduced data. *Neurocomputing*, 211:72–83, 2016.
- [8] Fazil Kaytez, M Cengiz Taplamacioglu, Ertugrul Cam, and Firat Hardalac. Forecasting electricity consumption: A comparison of regression analysis, neural networks and least squares support vector machines. *International Journal of Electrical Power & Energy Systems*, 67:431–438, 2015.
- [9] Inés M Galván, José M Valls, Alejandro Cervantes, and Ricardo Aler. Multi-objective evolutionary optimization of prediction intervals for solar energy forecasting with neural networks. *Information Sciences*, 418:363–382, 2017.
- [10] Yu Wang, Yinxing Shen, Shiwen Mao, Guanqun Cao, and Robert M Nelms. Adaptive learning hybrid model for solar intensity forecasting. *IEEE Transactions on Industrial Informatics*, 14(4):1635–1645, 2018.
- [11] Mahdi Khodayar, Saeed Mohammadi, Mohammad E Khodayar, Jianhui Wang, and Guangyi Liu. Convolutional graph autoencoder: A generative deep neural network for probabilistic spatio-temporal solar irradiance forecasting. *IEEE Transactions on Sustainable Energy*, 11(2):571–583, 2019.
- [12] Guang-Bin Huang, Qin-Yu Zhu, and Chee-Kheong Siew. Extreme learning machine: theory and applications. *Neurocomputing*, 70(1-3):489–501, 2006.
- [13] Ting Wang, Chun Sing Lai, Wing WY Ng, Keda Pan, Mingyang Zhang, Alfredo Vaccaro, and Loi Lei Lai. Deep autoencoder with localized stochastic sensitivity for short-term load forecasting. *International Journal of Electrical Power & Energy Systems*, 130:106954, 2021.
- [14] Songjian Chai, Ming Niu, Zhao Xu, Loi Lei Lai, and Kit Po Wong. Nonparametric conditional interval forecasts for pv power generation considering the temporal dependence. In *2016 IEEE Power and Energy Society General Meeting (PESGM)*, pages 1–5. IEEE, 2016.
- [15] Xiaomei Wu, Chun Sing Lai, Chenchen Bai, Loi Lei Lai, Qi Zhang, and Bo Liu. Optimal kernel elm and variational mode decomposition for probabilistic pv power prediction. *Energies*, 13(14):3592, 2020.
- [16] Amid Shahbazi, Jamshid Aghaei, Sasan Pirouzi, Miadreza Shafie-khah, and João PS Catalão. Hybrid stochastic/robust optimization model for resilient architecture of distribution networks against extreme weather conditions. *International Journal of Electrical Power & Energy Systems*, 126:106576, 2021.
- [17] Cristian Crisosto, Martin Hofmann, Riyadh Mubarak, and Gunther Seckmeyer. One-hour prediction of the global solar irradiance from all-sky images using artificial neural networks. *Energies*, 11(11):2906, 2018.
- [18] Yuxin Wen, Donna AlHakeem, Paras Mandal, Shantanu Chakraborty, Yuan-Kang Wu, Tomonobu Senjyu, Sumit Paudyal, and Tzu-Liang Tseng. Performance evaluation of probabilistic methods based on bootstrap and quantile regression to quantify pv power point forecast uncertainty. *IEEE Transactions on Neural Networks and Learning Systems*, 31(4):1134–1144, 2019.
- [19] Shikhar Srivastava and Stefan Lessmann. A comparative study of lstm neural networks in forecasting day-ahead global horizontal irradiance with satellite data. *Solar Energy*, 162:232–247, 2018.
- [20] Cheng Pan, Jie Tan, and Dandan Feng. Prediction intervals estimation of solar generation based on gated recurrent unit and kernel density estimation. *Neurocomputing*, 453:552–562, 2021.
- [21] Wei Liu and Yan Xu. Randomised learning-based hybrid ensemble model for probabilistic forecasting of pv power generation. *IET Generation, Transmission & Distribution*, 14(24):5909–5917, 2020.
- [22] Peerasak Wangsom, Pascal Bouvry, and Kittichai Lavangnananda. Extreme solutions nsga-iii (e-nsga-iii) for scientific workflow scheduling on cloud. In *2018 17th IEEE International Conference on Machine Learning and Applications (ICMLA)*, pages 1139–1146. IEEE, 2018.
- [23] Abbas Khosravi, Saeid Nahavandi, Doug Creighton, and Amir F Atiyya. Lower upper bound estimation method for construction of neural network-based prediction intervals. *IEEE Transactions on Neural Networks*, 22(3):337–346, 2010.
- [24] Can Wan, Zhao Xu, and Pierre Pinson. Direct interval forecasting of wind power. *IEEE Transactions on Power Systems*, 28(4):4877–4878, 2013.
- [25] Songjian Chai, Zhao Xu, and Wai Kin Wong. Optimal granule-based pis construction for solar irradiance forecast. *IEEE Transactions on Power Systems*, 31(4):3332–3333, 2015.
- [26] Daniel S Yeung, Jin-Cheng Li, Wing WY Ng, and Patrick PK Chan. Mlpnn training via a multiobjective optimization of training error and stochastic sensitivity. *IEEE Transactions on Neural Networks and Learning Systems*, 27(5):978–992, 2015.
- [27] Daniel S Yeung, Wing WY Ng, Defeng Wang, Eric CC Tsang, and Xi-Zhao Wang. Localized generalization error model and its application to architecture selection for radial basis function neural network. *IEEE Transactions on Neural Networks*, 18(5):1294–1305, 2007.
- [28] Wing WY Ng, Junjie Hu, Daniel S Yeung, Shaohua Yin, and Fabio Roli. Diversified sensitivity-based undersampling for imbalance classification problems. *IEEE Transactions on Cybernetics*, 45(11):2402–2412, 2014.
- [29] Xueli Zhang, Cankun Zhong, Jianjun Zhang, Ting Wang, and Wing WY Ng. Robust recurrent neural networks for time series forecasting. *Neurocomputing*, 526:143–157, 2023.
- [30] Ladislav Kocis and William J Whiten. Computational investigations of low-discrepancy sequences. *ACM Transactions on Mathematical Software (TOMS)*, 23(2):266–294, 1997.
- [31] Yvonne Gala, Ángela Fernández, Julia Díaz, and José R Dorronsoro. Hybrid machine learning forecasting of solar radiation values. *Neurocomputing*, 176:48–59, 2016.
- [32] The national renewable energy laboratory. <https://www.nrel.gov/gis/data-tools.html>. Accessed on 29 March 2021.
- [33] Nian Liu, Qifang Chen, Jie Liu, Xinyi Lu, Peng Li, Jinyong Lei, and Jianhua Zhang. A heuristic operation strategy for commercial building microgrids containing evs and pv system. *IEEE Transactions on Industrial Electronics*, 62(4):2560–2570, 2014.